



1N-37
393 807

TECHNICAL NOTE

D-1070

SKIN STRESSES IN AN INFLATED SPHERE
DURING IMPACT

By E. Dale Martin

Ames Research Center
Moffett Field, Calif.

PROPERTY

GOVERNMENT

NATIONAL AERONAUTICS AND SPACE ADMINISTRATION
WASHINGTON

August 1961

NATIONAL AERONAUTICS AND SPACE ADMINISTRATION

TECHNICAL NOTE D-1070

SKIN STRESSES IN AN INFLATED SPHERE

DURING IMPACT

By E. Dale Martin

SUMMARY

An analysis is made of the stresses in the skin of an inflated nonstretchable sphere during normal, nonrotating impact with a hard flat surface, assuming infinite modulus of elasticity in the skin and infinite propagation speed of stress waves. The analysis is further applied to the study of the inflated sphere landing vehicle containing a payload suspended at the center. Curves are presented showing the stress distributions during impact for cases corresponding to those calculated in previous reports in which the impact motion and payload landing performance capabilities of the landing vehicle have been studied.

It is found, assuming the force from the payload-suspension cords to be distributed continuously on the skin, that is, neglecting stress concentrations, that the skin stresses along a meridian are reduced by the presence of the suspended payload during impact, but that the maximum values of skin stress normal to a meridian are little affected.

INTRODUCTION

The use of an inflated sphere with a centrally supported payload package as a device for cushioning the high-speed impact of a payload has been studied in references 1 to 3. The impact motion and payload-landing performance were analyzed in reference 1. In reference 2 the internal-gas wave motion was studied and the effects of wave motion were shown to be important when the square of the ratio of impact velocity to speed of sound in the gas is not small. In reference 3, the payload-landing performance was calculated including consideration of the required mass of payload-suspension cords. These studies (refs. 1 to 3) indicated that in principle the use of an inflated sphere with the payload suspended at its center could, in fact, attenuate the impact acceleration to within allowable limits for hard landing of payloads. Impact velocities in the range from 500 to 1000 feet per second could be handled with maximum accelerations of the order of only several thousand g's for a sphere with a radius of the order of 10 feet (ref. 3).

In the previous studies of inflated-sphere impact the skin-stress distributions were not considered. Calculations were made based on an initial skin stress with the presumption that the subsequent stresses during the impact would not exceed the allowable ultimate value. However, precise information on maximum values of skin stresses during impact for various design conditions would be needed in an actual design.

When one considers the ramifications of the elastic wave phenomena and stress concentrations involved in an analysis of the stresses accompanying the impact motion of an actual vehicle of the type being studied, the complexity of the problem becomes evident. It is the purpose of this investigation to show the development of the stresses and their distribution during an impact with simplifications to allow a solution of the problem. Hopefully, the results will show the main features of the problem and will form a background for more detailed design studies, and may also serve as a guide in designing experiments to examine critical areas.

A
4
7
1

An analysis of the stresses in two directions at any point in the skin during the impact is presented. The various assumptions and approximations used are discussed prior to proceeding with the analysis. Results are shown corresponding to those of design cases calculated in previous reports, including cases in which there is no centrally supported payload and cases in which a payload is suspended in the center by cords. For the cases of centrally supported payloads, information concerning the cord-force distributions is also presented.

SYMBOLS

a	acceleration of the sphere center; $\frac{d^2y}{dt^2}$
\bar{a}	$\frac{r}{u_1^2} a$
c_v	specific heat of the inflating gas at constant volume
dS	area of differential skin element, ABCD (See sketch (c).)
f	cord force distribution (eq. (26))
g_e	gravitational acceleration on the earth, 32.17 ft/sec ²
K	proportionality constant (constant in θ but variable with time) for cord force distribution in $\theta^* \leq \theta \leq \frac{\pi}{2}$ (See eqs. (39).)
m	total mass of the system

$m()$	mass of a particular part of the system, depending on the subscript
n	number of earth g's maximum acceleration
p	pressure of the inflating gas
p_a	$\bar{p}_a p_1$, pressure of the atmosphere outside the sphere
p_c	$\bar{p}_c p_1$, force per unit area from the payload-suspension cords attached to the skin
\bar{p}	$\frac{p}{p_1}$
r	radius of the sphere
T	temperature of the inflating gas
t	time
u	velocity of the sphere center, $\frac{dy}{dt}$
\bar{u}	$\frac{u}{ u_1 }$
y	distance from the impact surface to the sphere center
\bar{y}	$\frac{y}{r}$
z	defined by equation (29)
α	$\arccos(-\bar{y})$
γ	ratio of specific heats of the inflating gas
δ	thickness of the sphere skin
ζ_a, ζ_b	functions of \bar{y} ; defined by equations (34) and (35)
θ	azimuthal angle from the top of the impacting sphere
θ^*	highest value of θ for which σ_θ has become zero at a given time
μ	defined by equation (27)
ξ	initial energy ratio, $\frac{mgcvT_1}{\frac{1}{2} m u_1^2}$
ρ	mass density

σ	stress
σ_θ	skin stress in the direction along a meridian
σ_ψ	skin stress normal to a meridian
ϕ_r	force in one payload-suspension cord at the sphere skin
ψ	polar angle (longitudinal coordinate)
$()^*$	value at $\theta = \theta^*$

Subscripts

o	value at $\theta = 0$
1	condition at the first instant of impact
2	condition at maximum compression of the gas which occurs when the velocity is zero
c	payload-suspension cords
g	inflating gas
p	centrally supported payload package
s	sphere skin
v	portion in motion with velocity u

ANALYSIS

Assumptions and Approximations

In the calculation of the impact motion of an inflated sphere membrane (refs. 1 to 3), a normal impact with no rotation is assumed. The "uniform gas" approximation for the internal gas pressure, which was used and discussed in reference 1, is retained in this analysis. Therefore, the internal gas pressure is a function only of time. The outside pressure is assumed to be constant at the value p_a .

It is assumed that the skin is flexible and nonstretchable. Then it is assumed that the part of the sphere skin not in contact with the impact surface retains its spherical shape (see ref. 1).

Also, because the skin material is assumed to be nonstretchable and thus to have an infinite modulus of elasticity, changes in stress due to the relaxation of stress in the meridional direction at the "impact circle" ($\theta = \alpha$) will propagate through the skin material infinitely fast in comparison to the impact speed. Therefore it is assumed that the effects of stress waves are negligible.

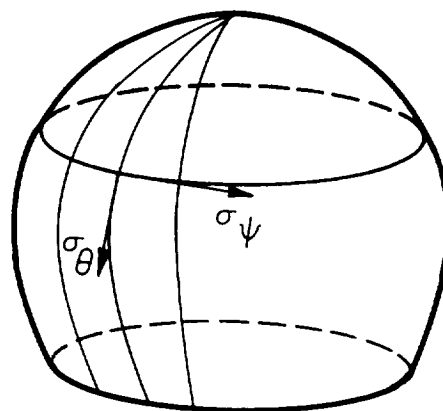
"Membrane theory" of shells is assumed to apply in the analysis of the skin stresses; moreover, it is assumed that the material cannot maintain compressive stresses. This is considered to be a very reasonable assumption for flexible materials, such as fabrics.

As in the prior analyses (ref. 3), the payload suspension cords are also assumed to be flexible and to have a very high modulus of elasticity. Therefore the parts of the cords in motion are assumed to have the same velocity as the sphere center.

The use of a large number of payload suspension cords is assumed, and the effects of stress concentrations due to cord attachments are neglected. The force from the cords is therefore assumed to be applied continuously over the skin surface. In the practical case the neglect of skin-stress concentrations may not be entirely realistic. Nevertheless, as the number of cords is increased, the assumed condition is approached. The use of the assumption of continuous force distribution enables one to estimate stresses, how the stresses change during impact, and where the maximum stresses will occur when the cords and payload are present.

Calculation of Skin Stresses

Equations for skin stress along a meridian, σ_θ , and skin stress normal to a meridian, σ_ψ .—Although several derivations of equations for stress in a spherical membrane can be found in the literature (e.g., refs. 4 and 5), brief, simple derivations are given here of the appropriate dynamic equations for the application to the particular type of motion of immediate concern. The tensile stress in the skin along a meridian (the meridian plane being perpendicular to the impact surface) is denoted as σ_θ . The tensile stress in the skin normal to a meridian is denoted as σ_ψ (see sketch (a)). The coordinates θ and ψ are, respectively, the azimuthal angle (latitudinal coordinate) and the polar angle

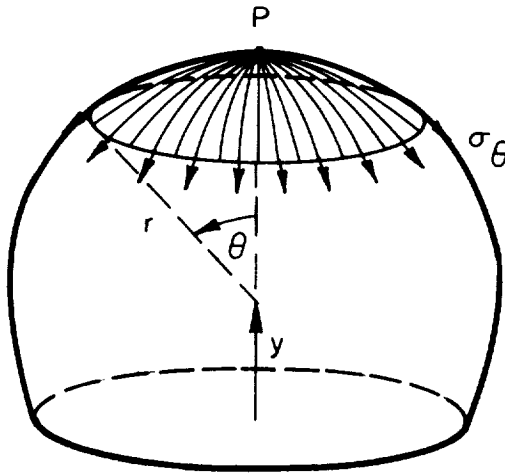


Sketch (a)

(longitudinal coordinate). This notation is used for convenience in relating the present study to the previous studies of the inflated sphere landing vehicle in references 1 and 3.

The stress equations are derived by applying Newton's second law of motion to various elements and portions of the sphere skin. The stresses σ_θ and σ_ψ will thus be obtained in terms of the skin properties, the acceleration of the sphere, and the force per unit area on the skin surface.

The meridional stress, σ_θ , can be most easily found by taking as the free body, to which Newton's law is applied, the portion of the skin



Sketch (b)

included between the pole, point P on sketch (b), and the angle θ (i.e., the shaded portion on sketch (b)), because σ_θ is the only stress normal to the boundary of this free body. If the mass of this portion of skin is denoted as m_θ , then

$$m_\theta = 2\pi r^2 \rho_s \delta (1 - \cos \theta) \quad (1)$$

Newton's law for the vertical motion of m_θ is then

$$m_\theta a = F_{p\theta} - F_{c\theta} - F_{\sigma\theta} \quad (2)$$

where a is the acceleration of the skin and of the sphere center, and where $-F_{p\theta}$, $F_{c\theta}$, and $F_{\sigma\theta}$ are the downward vertical forces on m_θ due, respectively, to external and internal gas pressures, to the payload suspension cords (in the case of centrally supported payload), and to the skin stress σ_θ . These forces are given, respectively, by:

$$F_{p\theta} = \int_0^\theta [(p - p_a) \cos \theta] [2\pi(r \sin \theta) r d\theta] = \pi r^2 (p - p_a) \sin^2 \theta \quad (3)$$

where p is assumed uniform over θ and p_a is constant,

$$F_{c\theta} = 2\pi r^2 \int_0^\theta p_c \sin \theta \cos \theta d\theta \quad (4)$$

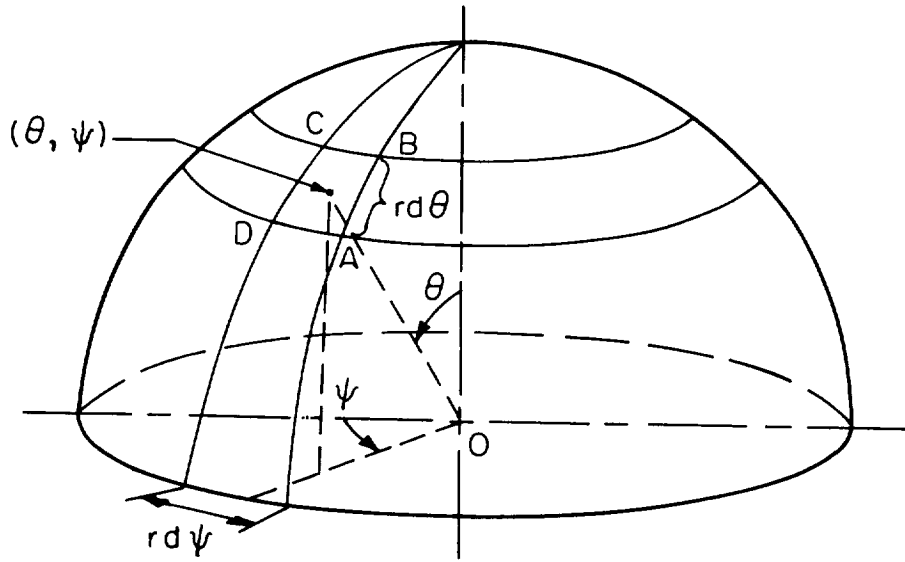
where p_c is the force per unit area from the cords attached to the skin, and

$$F_{\sigma\theta} = 2\pi r \delta \sigma_\theta \sin^2 \theta \quad (5)$$

Equation (2) then becomes

$$\frac{\sigma_\theta}{\rho_s} = \left(\frac{p_1 r}{\rho_s \delta} \right) \frac{\bar{p} - \bar{p}_a}{2} - \frac{u_1^2 \bar{a}}{1 + \cos \theta} - \left(\frac{p_1 r}{\rho_s \delta} \right) \frac{1}{\sin^2 \theta} \int_0^\theta \bar{p}_c \sin \theta \cos \theta d\theta \quad (6)$$

To find σ_ψ , the skin stress normal to a meridional plane, Newton's law may be written for the motion in the radial direction of the element of skin ABCD, bounded by the two meridians at $\psi - (1/2)d\psi$ and $\psi + (1/2)d\psi$, and by the two parallel circles at $\theta - (1/2)d\theta$ and $\theta + (1/2)d\theta$ (see sketch (c)). The lengths of the edges of this element are



Sketch (c)

$$\left. \begin{aligned}
 \widehat{AB} &= r \, d\theta \\
 \widehat{BC} &= r \sin \left(\theta - \frac{1}{2} d\theta \right) d\psi \\
 \widehat{CD} &= r \, d\theta \\
 \widehat{DA} &= r \sin \left(\theta + \frac{1}{2} d\theta \right) d\psi
 \end{aligned} \right\} \quad (7)$$

and the stresses in the skin acting normal to these edges are, respectively, $\sigma_\psi + (1/2)d\sigma_\psi$, $\sigma_\theta - (1/2)d\sigma_\theta$, $\sigma_\psi - (1/2)d\sigma_\psi$, and $\sigma_\theta + (1/2)d\sigma_\theta$. The components of these stresses acting toward the sphere center are, respectively,

$$\left. \begin{aligned}
 s_{AB} &= \left(\sigma_\psi + \frac{1}{2} d\sigma_\psi \right) \sin \left(\frac{1}{2} \sin \theta \, d\psi \right) \\
 s_{BC} &= \left(\sigma_\theta - \frac{1}{2} d\sigma_\theta \right) \sin \left(\frac{1}{2} d\theta \right) \\
 s_{CD} &= \left(\sigma_\psi - \frac{1}{2} d\sigma_\psi \right) \sin \left(\frac{1}{2} \sin \theta \, d\psi \right) \\
 s_{DA} &= \left(\sigma_\theta + \frac{1}{2} d\sigma_\theta \right) \sin \left(\frac{1}{2} d\theta \right)
 \end{aligned} \right\} \quad (8)$$

Therefore the radial force on the element ABCD due to the skin stresses is

$$F_\sigma = -(\widehat{AB}s_{AB}\delta + \widehat{BC}s_{BC}\delta + \widehat{CD}s_{CD}\delta + \widehat{DA}s_{DA}\delta) \quad (9)$$

The force per unit area normal to the skin surface is $p - p_a - p_c$. The surface area of the skin element is

$$dS = r^2 \sin \theta \, d\theta \, d\psi \quad (10)$$

and hence the radial force on the elemental surface due to gas pressure and cord forces is $(p - p_a - p_c)dS$. The mass of the skin element is $\rho_s \delta \, dS$ and its radial acceleration is $(du/dt)\cos \theta$. Newton's law for the radial motion of the element of skin ABCD then takes the form

$$\rho_s \delta \, dS \frac{du}{dt} \cos \theta = (p - p_a - p_c) dS + F_\sigma \quad (11)$$

Equation (11), along with (7), (8), (9), and (10), and the expressions

$$\sin \left(\frac{1}{2} d\theta \right) \approx \frac{1}{2} d\theta$$

$$\sin \left(\frac{1}{2} \sin \theta \, d\psi \right) \approx \frac{1}{2} \sin \theta \, d\psi$$

in equations (8) then lead to the following result:

$$\left. \begin{aligned} \frac{\sigma_\theta}{r} + \frac{\sigma_\psi}{r} &= \frac{(p - p_a - p_c) dS}{\delta \, dS} - \rho_s \frac{du}{dt} \cos \theta \\ &= \frac{\text{radial surface force}}{\text{unit volume}} + \frac{\text{radial acceleration force}}{\text{unit volume}} \end{aligned} \right\} \quad (12)$$

which is similar to familiar forms of the membrane-shell equation for a sphere as found in the literature. For present purposes, the following more convenient form may be written:

$$\frac{\sigma_\psi}{\rho_s} = \left(\frac{p_1 r}{\rho_s \delta} \right) (\bar{p} - \bar{p}_a) - \left(\frac{p_1 r}{\rho_s \delta} \right) \bar{p}_c - u_1^2 \bar{a} \cos \theta - \frac{\sigma_\theta}{\rho_s} \quad (13)$$

The two equations, (6) and (13), may then be used to calculate σ_θ and σ_ψ at any θ and at any time during the impact (where $\bar{p} - \bar{p}_a$ and \bar{a} are functions of time and \bar{p}_c is a function of θ and time). For the purpose of calculating σ_θ and σ_ψ corresponding to the numerical results calculated previously in references 1 and 3, equations (6) and (13) may be related to some expressions derived previously. The equation of motion used in references 1 and 3 is

$$\bar{a} = \frac{3(\gamma - 1)\xi}{8} \left(\frac{m}{m_v} \right) (1 - \bar{y}^2)(\bar{p} - \bar{p}_a) \quad (14)$$

where

$$\bar{p} - \bar{p}_a = \left(\frac{4}{2 + 3\bar{y} - \bar{y}^3} \right)^\gamma - \bar{p}_a \quad (15)$$

$$m_V = m_P + \frac{1}{2} m_S(1 + \bar{y}) + m_{CV} \quad (16)$$

and

$$\xi = \frac{m_S c_V T_1}{(1/2) m u_1^2} \quad (17)$$

The quantity m_{CV} is the part of the mass of the payload suspension cords in motion with velocity $u = dy/dt$. In reference 1 m_{CV} was neglected or assumed to be zero; in the text and appendix of reference 3 expressions for m_{CV} as functions of \bar{y} were derived for the cases of constant-area cords and exponentially tapered cords, respectively. An expression for the gas pressure term in equations (6) and (13) may be obtained by putting equation (14) into the form:

$$\left(\frac{p_1 r}{\rho_S \delta}\right) (\bar{p} - \bar{p}_a) = \frac{4 u_1^2 \bar{a}}{1 - \bar{y}^2} \left(\frac{m_V}{m_S}\right) \quad (18)$$

Thus equations (6) and (13) may be written:

$$\frac{\sigma_\theta}{\rho_S} = u_1^2 \bar{a} \left[\left(\frac{2}{1 - \bar{y}^2} \right) \frac{m_V}{m_S} - \left(\frac{1}{1 + \cos \theta} \right) \right] - \frac{1}{\sin^2 \theta} \left(\frac{p_1 r}{\rho_S \delta} \right) \int_0^\theta \bar{p}_c \sin \theta \cos \theta \, d\theta \quad (19)$$

$$\frac{\sigma_\psi}{\rho_S} = u_1^2 \bar{a} \left[\left(\frac{4}{1 - \bar{y}^2} \right) \frac{m_V}{m_S} - \cos \theta \right] - \left(\frac{p_1 r}{\rho_S \delta} \right) \bar{p}_c - \frac{\sigma_\theta}{\rho_S} \quad (20)$$

Skin stresses for case of sphere without payload.— In the case of an inflated nonstretchable sphere membrane containing only the inflating gas and no centrally supported payload (but possibly having instrumentation printed on and/or attached to the skin, which is taken into account in determining ρ_S), equations (19) and (20) may be used by setting \bar{p}_c identically to zero. Thus

$$\left(\frac{\sigma_\theta}{\rho_S}\right)_{\substack{m_P=0 \\ m_C=0}} = u_1^2 \bar{a} \left[\left(\frac{2}{1 - \bar{y}^2} \right) \frac{m_V}{m_S} - \left(\frac{1}{1 + \cos \theta} \right) \right] \quad (21)$$

and

$$\left(\frac{\sigma_\psi}{\rho_S}\right)_{\substack{m_P=0 \\ m_C=0}} = u_1^2 \bar{a} \left[\left(\frac{4}{1 - \bar{y}^2} \right) \frac{m_V}{m_S} - \cos \theta \right] - \left(\frac{\sigma_\theta}{\rho_S}\right)_{\substack{m_P=0 \\ m_C=0}} \quad (22)$$

The results from reference 1 for $m_p = 0$ may be used in the calculation, since

$$\left(\frac{m_v}{m_s}\right)_{m_p=0, m_c=0} = \frac{1}{2} (1 + \bar{y}) \quad (23)$$

Distribution of cord forces on the skin and skin stresses in sphere containing centrally supported payload.- In the cases of impact of the sphere landing vehicle with centrally supported payload, the terms in equations (19) and (20) representing the forces from the suspension cords on the skin remain to be determined. For some cases the cord-force distribution is directly related to, and coupled with, the skin-stress distribution. This relationship must therefore also be derived. As a result of this derivation, the parameter μ , which represents the integrated effect of the cord-force distribution over the sphere, and in terms of which the results in the previous studies (ref. 3, text and appendix) were found, will then be determined.

The force in one cord at $\eta = r$ (at the skin) is denoted in the text of reference 3 by the symbol ϕ . In the appendix of reference 3, the symbol ϕ' is used to denote the force in one cord as a function of radial distance η . Let ϕ_r denote either the ϕ of reference 3 or the value of ϕ' at $\eta = r$ in the appendix of reference 3. The quantity of interest in the equations is

$$\left(\frac{p_1 r}{\rho_s \delta}\right) \bar{p}_c = \left(\frac{p_1 r}{\rho_s \delta}\right) \left(\frac{N_c \phi_r}{4\pi r^2 p_1}\right) = \left(\frac{r}{m_s}\right) N_c \phi_r \quad (24)$$

where N_c is the total number of payload suspension cords attached to the skin and hence $N_c/4\pi r^2$ is the number per unit area. The forces in the cords are assumed to be zero before impact. It was shown in the text and appendix of reference 3, for constant-area and exponentially tapered cords, respectively, that

$$N_c \phi_r = \left(\frac{2}{\mu}\right) (m_p + m_{cv}) a f \quad (25)$$

where f is the cord-force distribution over θ :

$$f = \frac{\phi_r}{\phi_{r0}} \quad (26)$$

and where μ is defined by

$$\mu = \int_0^{\pi/2} f \sin \theta \cos \theta \, d\theta \quad (27)$$

Combining equations (24) and (25) and making use also of equation (16) then yield the result

$$\left(\frac{p_1 r}{\rho_s \delta}\right) \bar{p}_c = u_1^2 \bar{a} \left[\frac{m_V}{m_S} - \left(\frac{1 + \bar{y}}{2} \right) \right] \frac{2f}{\mu} \quad (28)$$

After substitution of equation (28) and defining

$$z = \int_0^\theta f \sin \theta \cos \theta \, d\theta \quad (29)$$

the stress equations, (19) and (20), become

$$\frac{\sigma_\theta}{\rho_s} = u_1^2 \bar{a} \left\{ \left(\frac{2}{1 - \bar{y}^2} \right) \frac{m_V}{m_S} - \left(\frac{1}{1 + \cos \theta} \right) - \frac{2}{\sin^2 \theta} \left[\frac{m_V}{m_S} - \left(\frac{1 + \bar{y}}{2} \right) \right] \frac{z}{\mu} \right\} \quad (30)$$

$$\frac{\sigma_\psi}{\rho_s} = u_1^2 \bar{a} \left\{ \left(\frac{4}{1 - \bar{y}^2} \right) \frac{m_V}{m_S} - \cos \theta - 2 \left[\frac{m_V}{m_S} - \left(\frac{1 + \bar{y}}{2} \right) \right] \frac{f}{\mu} \right\} - \frac{\sigma_\theta}{\rho_s} \quad (31)$$

Values of m_S/m , u_1 , and the functions m_V/m and \bar{a} , which depend on \bar{y} , have been calculated previously for several cases in reference 3. The quantities f , z , and μ in equations (30) and (31) are, as yet, undetermined for the general case. It is shown in reference 3 that, as long as $(\sigma_s)_0$ remains greater than zero, f is given by

$$\left. \begin{aligned} f &= \cos \theta, & [0 \leq \theta \leq \frac{\pi}{2}, (\sigma_s)_0 > 0] \\ f &= 0, & \left(\theta > \frac{\pi}{2} \right) \end{aligned} \right\} \quad (32)$$

The condition that σ_s be greater than zero at $\theta = 0$ requires that

$$2\zeta_a - 6\zeta_b > 1 \quad (33)$$

in equation (30), where

$$\zeta_a = \zeta_a(\bar{y}) = \left(\frac{2}{1 - \bar{y}^2} \right) \frac{m_V}{m_S} \quad (34)$$

and

$$\xi_b = \xi_b(\bar{y}) = \frac{m_V}{m_S} - \left(\frac{1 + \bar{y}}{2} \right) \quad (35)$$

Therefore, if the inequality (33) is satisfied, then equations (27), (29), and (32) give the following expressions which may be used in equations (30) and (31) for complete evaluation of σ_θ/ρ_S and σ_ψ/ρ_S over θ at a given value of \bar{y} :

$$\text{For } (\sigma_S)_0 > 0, \left\{ \begin{array}{ll} \frac{f}{\mu} = 3 \cos \theta, & \left(0 \leq \theta \leq \frac{\pi}{2} \right) \\ \frac{f}{\mu} = 0, & \left(\frac{\pi}{2} \leq \theta \leq \alpha \right) \\ \frac{z}{\mu} = 1 - \cos^3 \theta, & \left(0 \leq \theta \leq \frac{\pi}{2} \right) \\ \frac{z}{\mu} = 1, & \left(\frac{\pi}{2} \leq \theta \leq \alpha \right) \\ \mu = \frac{1}{3} \end{array} \right\} \quad (36)$$

where

$$\alpha = \arccos(-\bar{y}) \quad (37)$$

For all cases, for some period of time at the beginning of the impact, $(\sigma_S)_0 > 0$ so that the inequality (33) holds, and equations (36) may be used in (30) and (31). In some cases this condition will exist until $t = t_2$, and thus μ_2 will have the value $1/3$. For other cases, because the maximum force per unit area, or "pressure" from the cords occurs at $\theta = 0$ (eqs. (32)), the skin stress at $\theta = 0$ may be reduced to zero at some time during the impact as the acceleration increases. As explained in reference 3, before $(\sigma_S)_0$ becomes zero the upper hemisphere can be considered to be a rigid shell because it does not flex, and the cord-force distribution is not affected by the skin stresses; but, after $(\sigma_S)_0$ becomes zero, the upper hemisphere can no longer be considered to be entirely a rigid shell. The cord-force distribution then changes so that $(\sigma_S)_0$ remains zero and does not become negative. As the acceleration increases further after the first instant that $(\sigma_S)_0$ has become zero, the meridional stress in the skin a small distance from $\theta = 0$ also becomes zero. But $(\sigma_S)_0$ must remain at zero because if the stress became negative, the skin would flex, thus reducing the cord force, and the cause of the reduction in skin stress would be removed. Thus the region of zero

meridional skin stress grows with increase in acceleration but keeps its spherical shape. At all points in the upper hemisphere where the skin stress is still greater than zero, the skin can still be considered to be a nonflexing rigid shell, and the forces in the cords continue to be distributed proportional to $\cos \theta$ because of the assumption of high modulus of elasticity in the skin (see ref. 3). Denote θ^* as the highest value of θ for which the meridional skin stress, σ_θ , has become zero. Then, after $(\sigma_s)_0$ has become zero,

$$\sigma_\theta = 0 \quad \text{in } 0 \leq \theta \leq \theta^* \quad (38)$$

but

$$\sigma_\theta > 0 \quad \text{in } \theta^* < \theta < \alpha$$

and, as explained above,

$$\left. \begin{aligned} f &= K \cos \theta & \text{in } \theta^* \leq \theta \leq \frac{\pi}{2} \\ f &= 0 & \text{for } \theta > \frac{\pi}{2} \end{aligned} \right\} \quad (39)$$

Condition (38) will be used to find f in $(0 \leq \theta \leq \theta^*)$. Both θ^* and K are as yet undetermined; therefore another condition is needed along with equations (39) to determine θ^* and K . It is the condition of continuity of f at $\theta = \theta^*$, which can be reasoned as follows: During the impact the acceleration increases continuously with time, causing the cord forces to increase continuously thus reducing the skin stress, σ_θ , at a point continuously until it becomes zero; that is, until θ^* reaches that point. Therefore σ_θ is also continuous over θ at θ^* and hence, considering equation (30),

$$f \text{ is continuous at } \theta = \theta^* \quad (40)$$

To find f in $0 \leq \theta \leq \theta^*$, substitute condition (38) into equation (30). Thus

$$\zeta_a \sin^2 \theta - 1 + \cos \theta - 2\zeta_b \frac{z}{\mu} = 0 \quad (41)$$

where ζ_a and ζ_b are given by equations (34) and (35). Equation (41) may then be differentiated with respect to θ to obtain:

$$\frac{f}{\mu} = \frac{\zeta_a}{\zeta_b} - \frac{1}{2\zeta_b \cos \theta}, \quad (0 \leq \theta \leq \theta^*) \quad (42a)$$

Directly from equation (41) can be obtained:

$$\frac{z}{\mu} = \frac{\zeta_a}{2\zeta_b} \sin^2 \theta - \frac{1}{2\zeta_b} (1 - \cos \theta), \quad (0 \leq \theta \leq \theta^*) \quad (42b)$$

As noted above, equations (39) and condition (40) will be used to evaluate θ^* and K for use in the interval $\theta^* \leq \theta \leq (\pi/2)$. An expression for K/μ can be obtained by applying condition (40) to equations (39) and (42a):

$$\frac{K}{\mu} = \frac{\zeta_a}{\zeta_b} \frac{1}{\cos \theta^*} - \frac{1}{2\zeta_b \cos^2 \theta^*} \quad (43)$$

A second expression for K/μ can be found by writing equation (27) as

$$1 = \int_0^{\theta^*} \frac{f}{\mu} \sin \theta \cos \theta \, d\theta + \int_{\theta^*}^{\pi/2} \frac{f}{\mu} \sin \theta \cos \theta \, d\theta \quad (44)$$

and by substituting into this equations (39) and (42a). Thus

$$\frac{K}{\mu} = \frac{3}{\cos^3 \theta^*} \left[1 - \frac{\zeta_a}{2\zeta_b} \sin^2 \theta^* + \frac{1}{2\zeta_b} (1 - \cos \theta^*) \right] \quad (45)$$

Equations (43) and (45) may then, of course, be combined to solve for θ^* as the angle whose cosine is

$$\cos \theta^* = \frac{1}{\zeta_a} \left[1 + \sqrt{1 - 3\zeta_a(1 - \zeta_a + 2\zeta_b)} \right] \quad (46)$$

The value of K/μ is determined by substituting equation (46) into (43). The quantities of interest in the stress equation are f/μ and z/μ . From equations (39),

$$\frac{f}{\mu} = \frac{K}{\mu} \cos \theta, \quad \left(\theta^* \leq \theta \leq \frac{\pi}{2} \right) \quad (47)$$

where K/μ is known from equations (43) and (46). From equation (29),

$$\frac{z}{\mu} = \left(\frac{z}{\mu} \right)^* + \int_{\theta^*}^{\theta} \frac{f}{\mu} \sin \theta \cos \theta \, d\theta \quad (48)$$

where, from equation (42b),

$$\left(\frac{z}{\mu}\right)^* = \frac{\zeta_a}{2\zeta_b} \sin^2 \theta^* - \frac{1}{2\zeta_b} (1 - \cos \theta^*) \quad (49)$$

Substitution of equation (47) into equation (48) gives the result

$$\frac{z}{\mu} = \left(\frac{z}{\mu}\right)^* + \frac{1}{3} \left(\frac{K}{\mu}\right) (\cos^3 \theta^* - \cos^3 \theta), \quad \left(\theta^* \leq \theta \leq \frac{\pi}{2}\right) \quad (50)$$

In the interval $\pi/2 \leq \theta \leq \alpha$ the expressions for f/μ and z/μ are, of course,

$$\frac{f}{\mu} = 0, \quad \left(\frac{\pi}{2} \leq \theta \leq \alpha\right) \quad (51a)$$

$$\frac{z}{\mu} = 1, \quad \left(\frac{\pi}{2} \leq \theta \leq \alpha\right) \quad (51b)$$

It remains to determine μ for the cases in which $(\sigma_s)_0$ becomes zero. By definition, the value of f at $\theta = 0$ is

$$f_0 = 1 \quad (52)$$

Thus

$$\mu = \frac{f_0}{(f/\mu)_0} = \frac{1}{(f/\mu)_0} \quad (53)$$

The result of substituting equation (42a) into (53) is

$$\mu = \frac{\zeta_b}{\zeta_a - (1/2)}, \quad [(\sigma_s)_0 = 0] \quad (54)$$

The parameter K is then determined from equations (43) and (54):

$$K = \frac{1}{\zeta_a - (1/2)} \left(\frac{\zeta_a}{\cos \theta^*} - \frac{1}{2 \cos^2 \theta^*} \right) \quad (55)$$

To summarize the above development: If, at a given time or given value of \bar{y} , the inequality (33) is satisfied, then $(\sigma_s)_0 > 0$, $\mu = 1/3$, and f/μ and z/μ are given by equations (36). If the inequality (33) is not satisfied, then $(\sigma_s)_0 = 0$, μ is given by equation (54), θ^* is found

from equation (46), K/μ from (43), and f/μ and z/μ are given by equations (42a), (42b), (47), (49), (50), (51a), and (51b). Thus equations (30) and (31) are now completely determined and an expression for the parameter μ has been derived.

DISCUSSION OF RESULTS

The complete distribution of skin stress in the θ and ψ directions at all points in the skin and at all times during the impact can be obtained from the equations derived in the preceding analysis, both for cases in which there is no centrally supported payload and for cases in which a payload is suspended by radial cords. It is easily shown from equation (30) for σ_θ/ρ_s that, at $\theta = \alpha$, σ_θ is identically zero. This exhibits the fact that there can be no tensile stress along a meridian in the skin at the part of the skin in contact with the ground where the collapse is taking place. It can also be demonstrated by combining the expressions for σ_θ/ρ_s and σ_ψ/ρ_s (eqs. (30) and (31)) that at $\theta = 0$, $\sigma_\theta = \sigma_\psi$. At $\theta = 0$, of course, the stress has the same value in any direction tangent to the skin.

The distribution of skin stress along a meridian, σ_θ , over θ at different times during the impact is shown for five different cases in figure 1. These cases correspond to specific cases for which the impact motion was calculated in previous studies. For the case of no centrally supported payload (fig. 1(a)), after the first instant of impact σ_θ is highest at $\theta = 0$ and is zero at $\theta = \alpha$. As \bar{y} decreases from 1.0 to \bar{y}_2 ($\bar{y}_2 = 0$ in this case), $(\sigma_s/\rho_s)_{\theta=0}$ first decreases from 10^8 ft²/sec², then increases to 1.329×10^8 ft²/sec². In figures 1(b) through (e) are shown four cases for which a payload is centrally suspended by cords. In these cases it is seen that σ_θ decreases at all points as the impact progresses. Obviously, one effect of the cord forces is to decrease the force per unit area acting normal to the skin and thus to decrease the stress in the skin, at least in the vertical, or meridional, plane.

Figure 2 shows the distribution of skin stress normal to a meridian, σ_ψ , over θ at various times during the impact for the same cases plotted in figure 1. It is seen that the maximum value of σ_ψ in the sphere occurs adjacent to the part of the skin which is collapsing, that is, at $\theta = \alpha$, and the maximum in time occurs at the end of the impact, when $\bar{y} = \bar{y}_2$, for all cases, whether or not there is a payload suspended at the center. Although the maximum values of σ_ψ are evidently not too greatly affected by the magnitude of m_p/m , or by whether or not a suspended payload is present, they are affected by varying \bar{y}_2 .

The maximum stress for a given case is in the ψ direction (normal to a meridian) at $\theta = \alpha$ and at $\bar{y} = \bar{y}_2$. Values of $(\sigma_\psi/\sigma_{s1})_{\theta=\alpha, \bar{y}=\bar{y}_2}$ are

shown in figure 3 for spheres containing constant-area cords for various design cases corresponding to u_1 , as calculated in reference 3 (part (a) only). The calculations for figure 3 were made from the following equation, which is derived from equation (31) with the conditions $\bar{y} = \bar{y}_2$, $\theta = \alpha$, and using the fact that when $\bar{y} = \bar{y}_2$, $u_1^2 \bar{a} = (nr)g_e$:

$$\left(\frac{\sigma_\psi}{\rho_s}\right)_{\substack{\theta=\alpha \\ \bar{y}=\bar{y}_2}} = (nr)g_e \left[\left(\frac{4}{1 - \bar{y}^2} \right) \frac{m_{v2}}{m_s} + \bar{y}_2 \right] \quad (56)$$

Evidently the maximum values of σ_s can be quite high — as high as 5.6 times the initial skin stress — for $\bar{y}_2 = 0$ (fig. 3). The maximum value of σ_s is significantly reduced by having \bar{y}_2 greater than zero.

As pointed out earlier, the skin-stress distributions and the cord-force distributions are interdependent. Therefore, in the process of solving the skin-stress distributions, the cord-force distributions have also been determined. In figure 4 are presented examples of the cord-force distributions over θ when $\bar{y} = \bar{y}_2$ for four of the design cases used in figures 1 and 2, and also for those cases in which the skin stress at $\theta = 0$ never reaches zero, that is, the cases where f is a cosine function for the entire process, with the result that $\mu_2 = 1/3$. In figure 5 the values of μ_2 , for the same cases for which maximum stresses were calculated in figure 3(a), are given. From these values of μ_2 and the values of $\mu_2(\sigma_{c2}/\rho_c)$ for which the design parameters were calculated can be found the appropriate values of σ_{c2}/ρ_c . It is observed from figure 5 that, for those cases where m_p/m is high, μ_2 actually does approach the value $1/2$, as was reasoned physically in reference 3.

CONCLUDING REMARKS

It has been shown that the maximum skin stress in a nonstretchable inflated sphere during impact occurs in a direction normal to a meridian at the impact circle — that is, adjacent to the part of the skin which is collapsing — at the instant of maximum compression of the gas and maximum acceleration of the sphere. The maximum stress depends mainly on the initial stress, and on the final volume ratio of the impacting sphere (for no outside atmospheric pressure). When the sphere compresses to a hemisphere, the maximum stress can be five times as large as the initial stress for the cases considered.

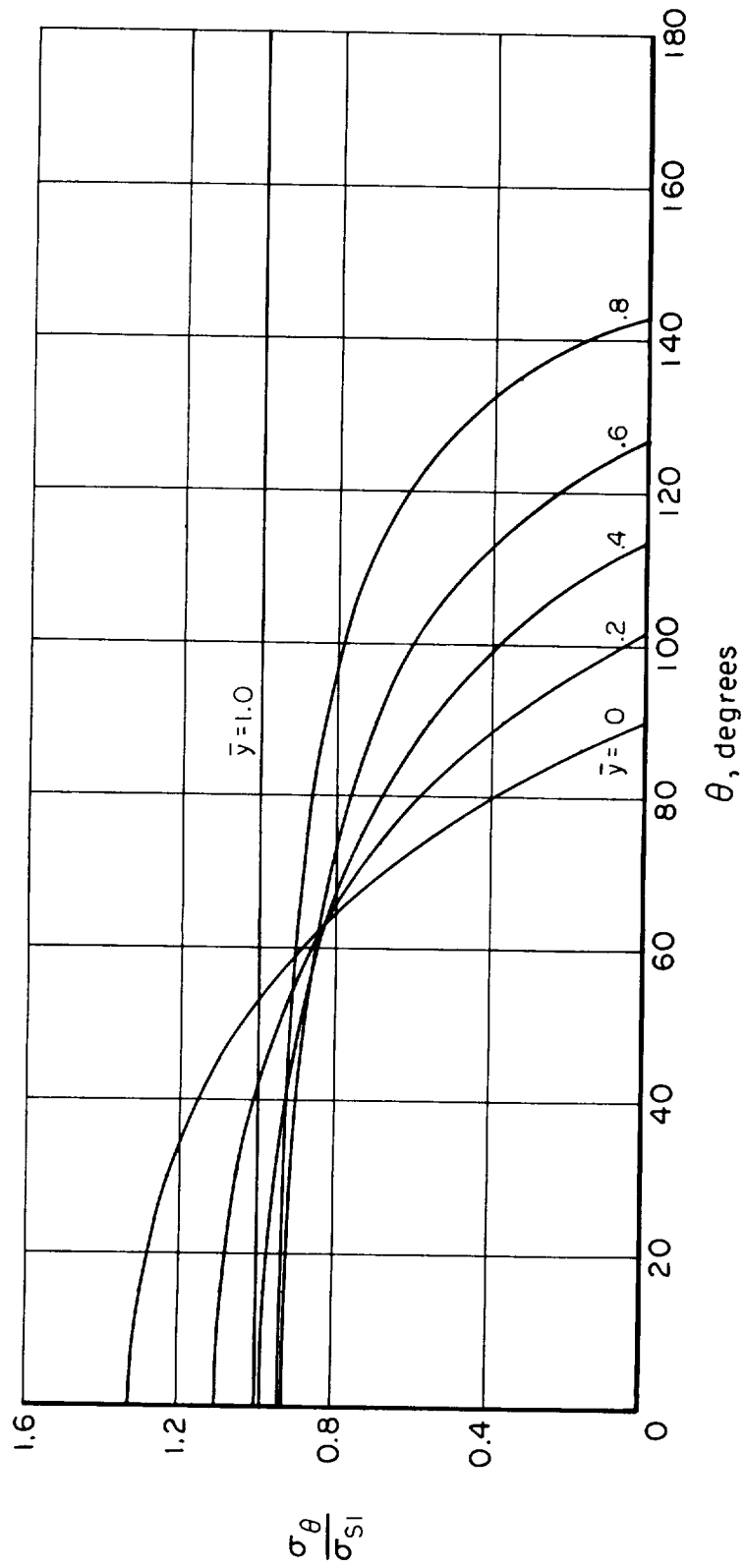
The distributions of stress in the meridional direction and stress normal to a meridian over the sphere are affected by the suspension of a payload at the center of the sphere. When the distribution of force per unit area due to the payload suspension cords is assumed to be continuous over the skin, the skin stress along a meridian is found to be greatly decreased in many cases by the effect of the cord forces. Although the

shape of the distribution curve of stress normal to a meridian is changed by the presence of a centrally supported payload, the maximum value is little affected.

Ames Research Center
National Aeronautics and Space Administration
Moffett Field, Calif., June 9, 1961

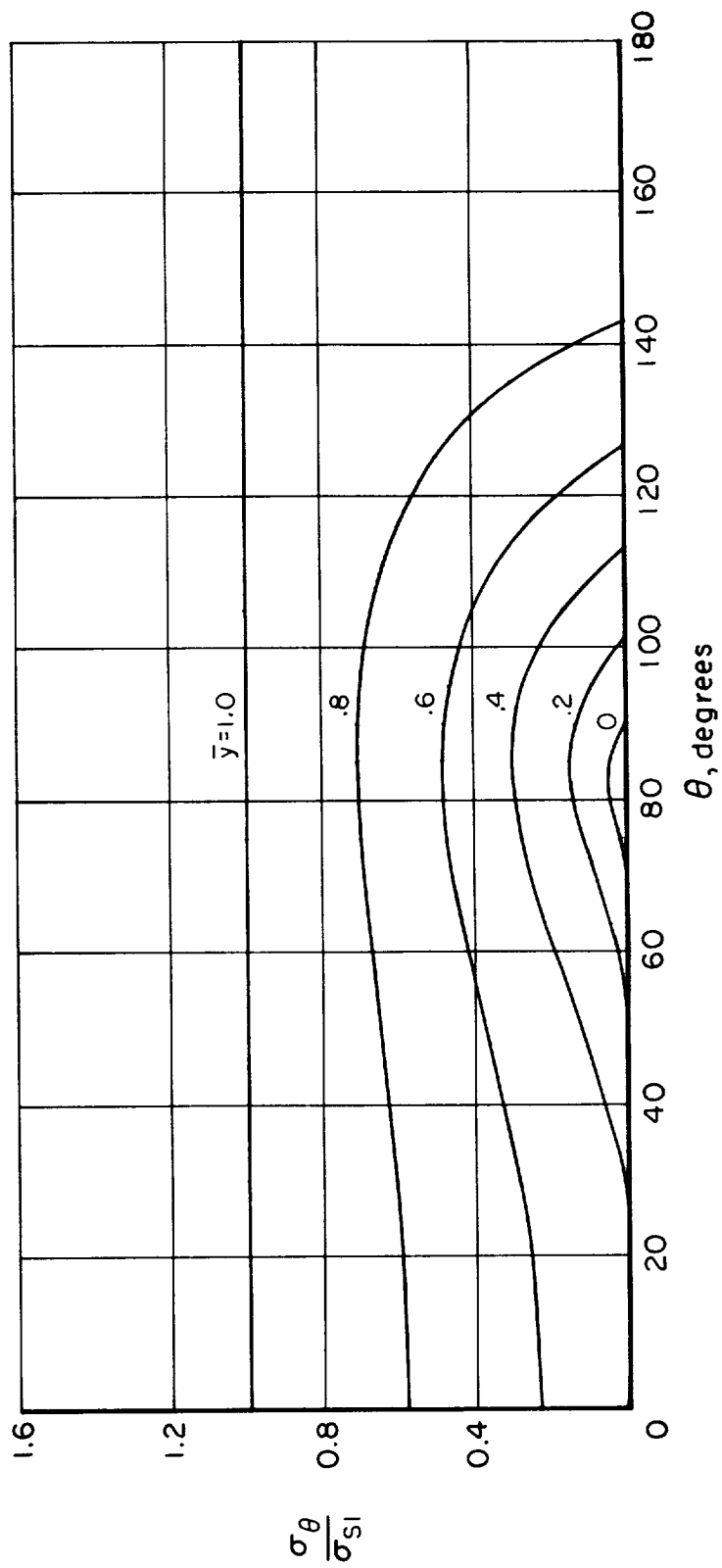
REFERENCES

1. Martin, E. Dale, and Howe, John T.: An Analysis of the Impact Motion of an Inflated Sphere Landing Vehicle. NASA TN D-314, 1960.
2. Howe, John T., and Martin, E. Dale: Gas Dynamics of an Inflated Sphere Striking a Surface. NASA TN D-315, 1960.
3. Martin, E. Dale: A Design Study of the Inflated Sphere Landing Vehicle, Including the Landing Performance and the Effects of Deviations From Design Conditions. NASA TN D-692, 1961.
4. Timoshenko, S.: Theory of Plates and Shells. McGraw-Hill Book Company, Inc., N.Y., 1940.
5. Flügge, Wilhelm: Statik und Dynamik der Schalen. Berlin, Springer-Verlag, 1957.



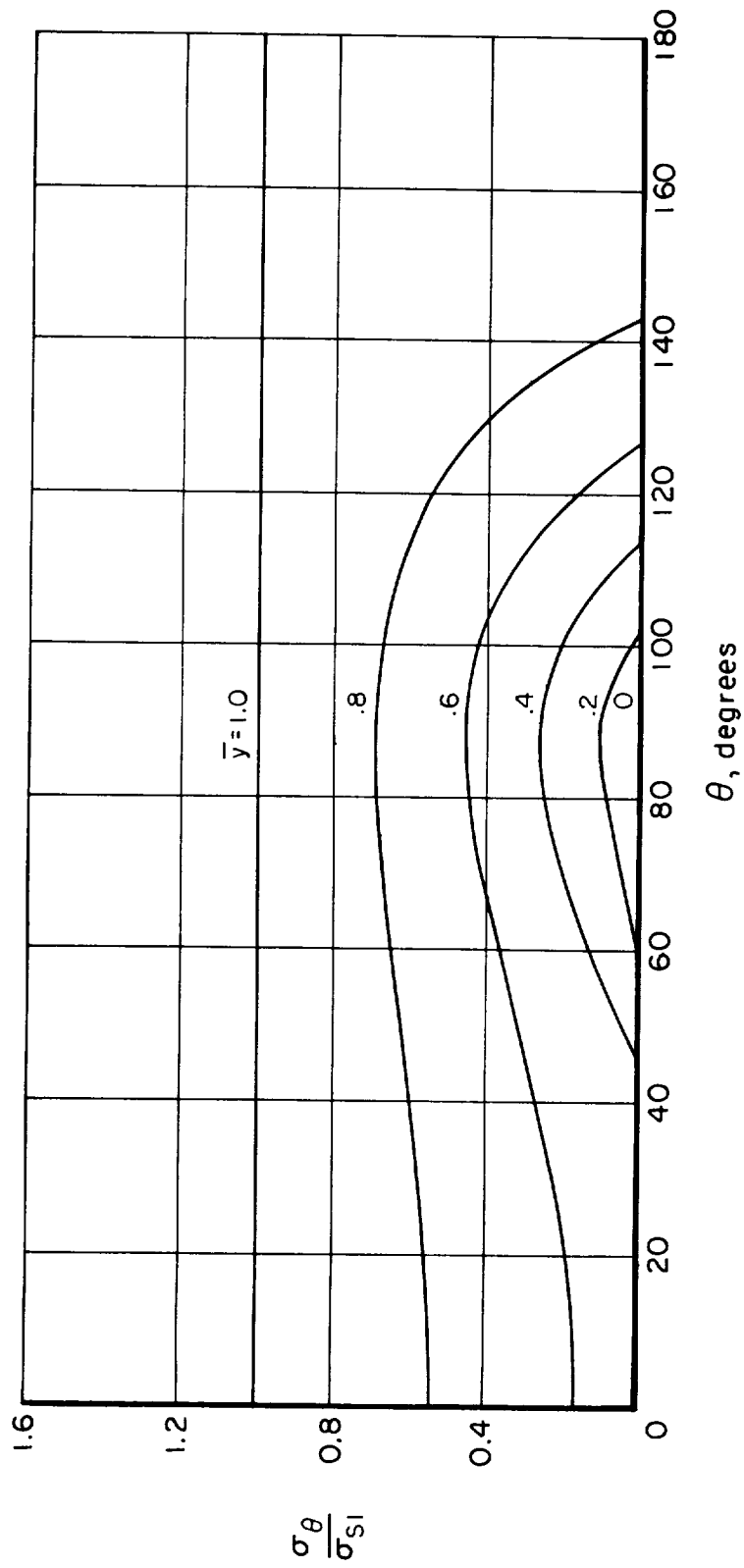
(a) $m_p/m = 0$, $m_c/m = 0$, $\bar{y}_2 = 0$ ($-u_1 = 1296.9$ ft/sec)

Figure 1.- Skin stress along a meridian (hydrogen inflating gas, $\bar{p}_a = 0$, $T_1 = 500^\circ$ R, $\sigma_{s1}/\rho_s = 10^6$ ft²/sec²).



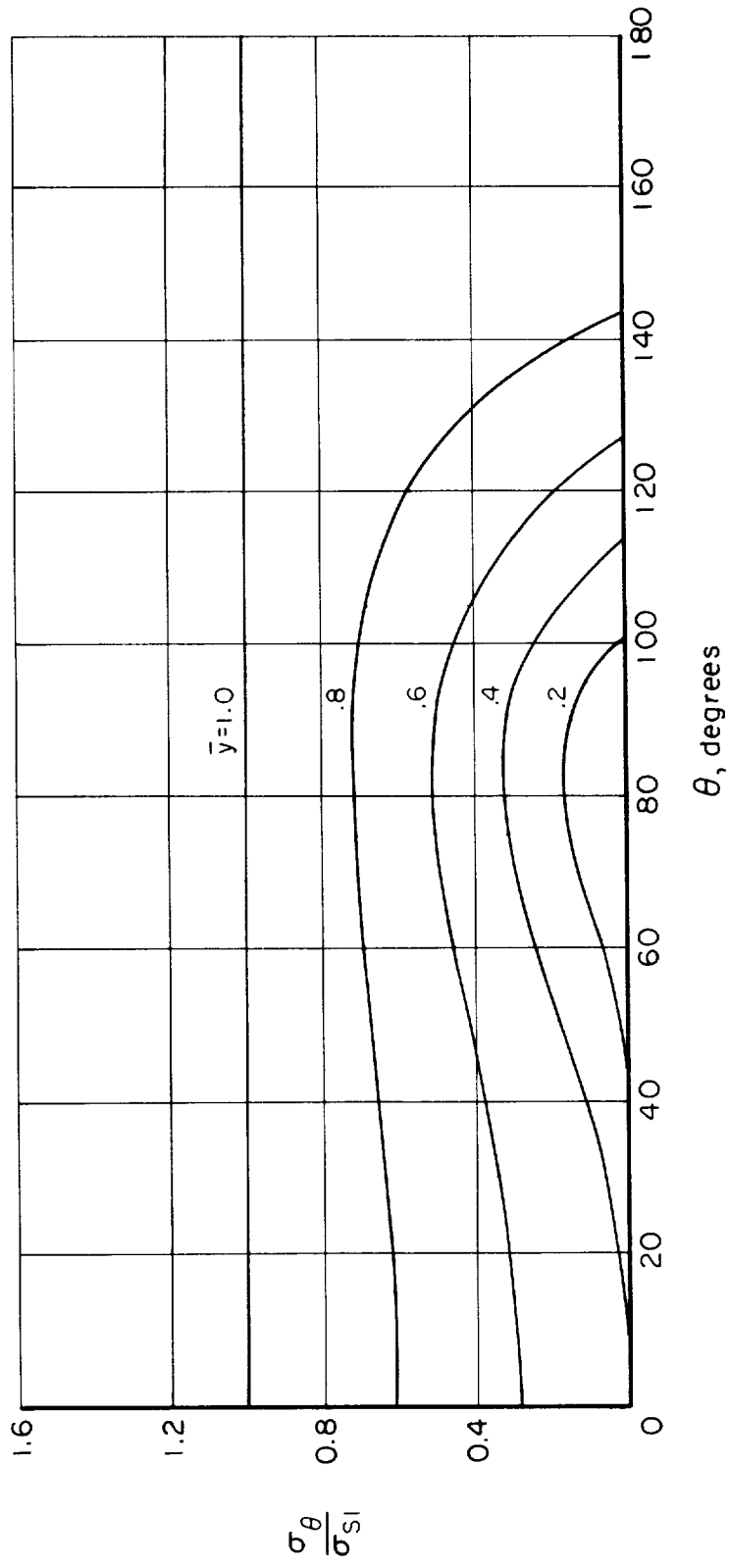
(b) Constant-area cords, $\mu_2(\sigma_{c2}/\rho_c) = 1.6 \times 10^6 \text{ ft}^2/\text{sec}^2$, $m_p/m = 0.4$, $\bar{y}_2 = 0$ ($-u_1 = 567.7 \text{ ft/sec}$).

Figure 1.- Continued.



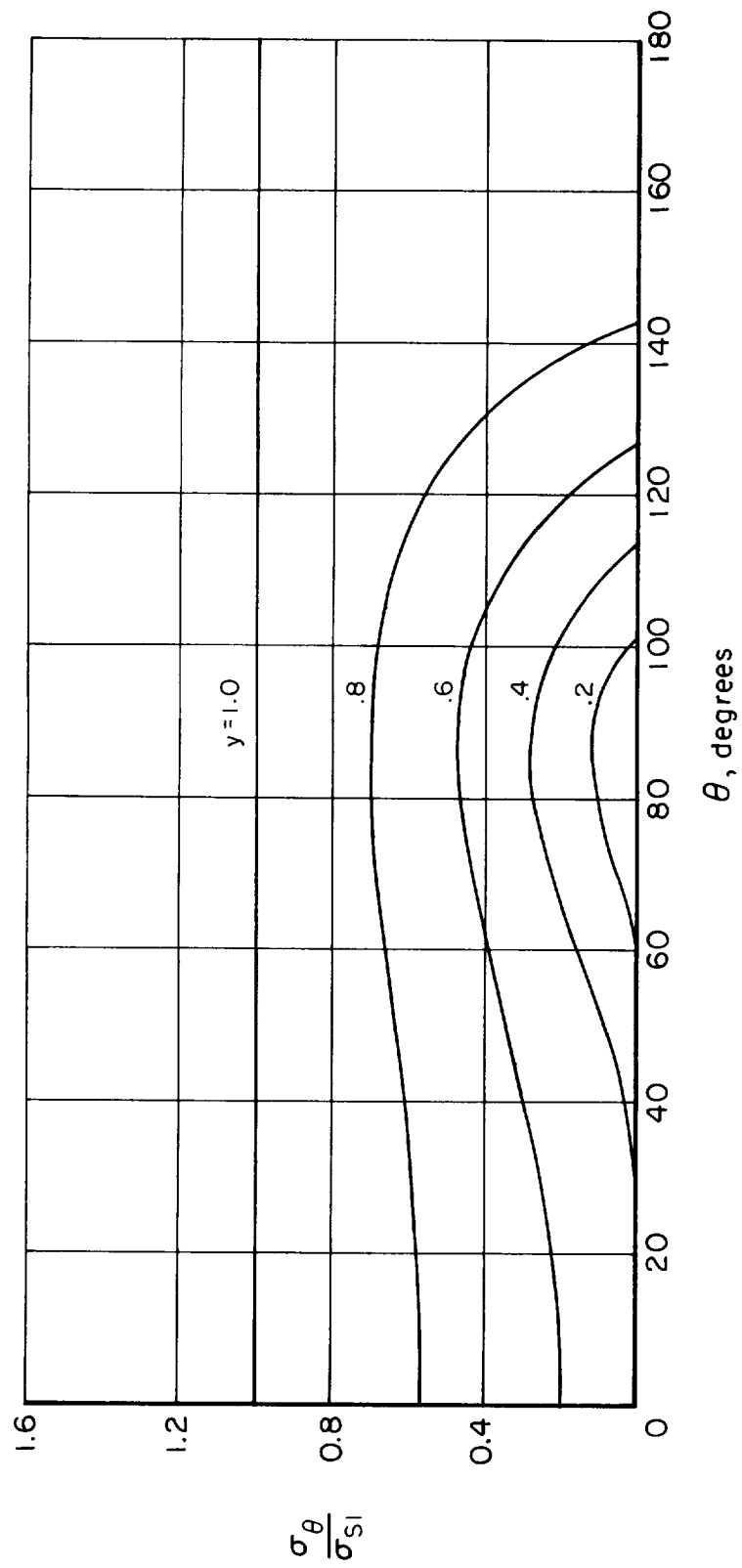
(c) Constant-area cords, $\mu_2(\sigma_{c2}/\rho_c) = 1.6 \times 10^6 \text{ ft}^2/\text{sec}^2$, $m_p/m = 0.6$, $\bar{y}_2 = 0$ ($-u_1 = 435.1 \text{ ft/sec}$).

Figure 1.- Continued.



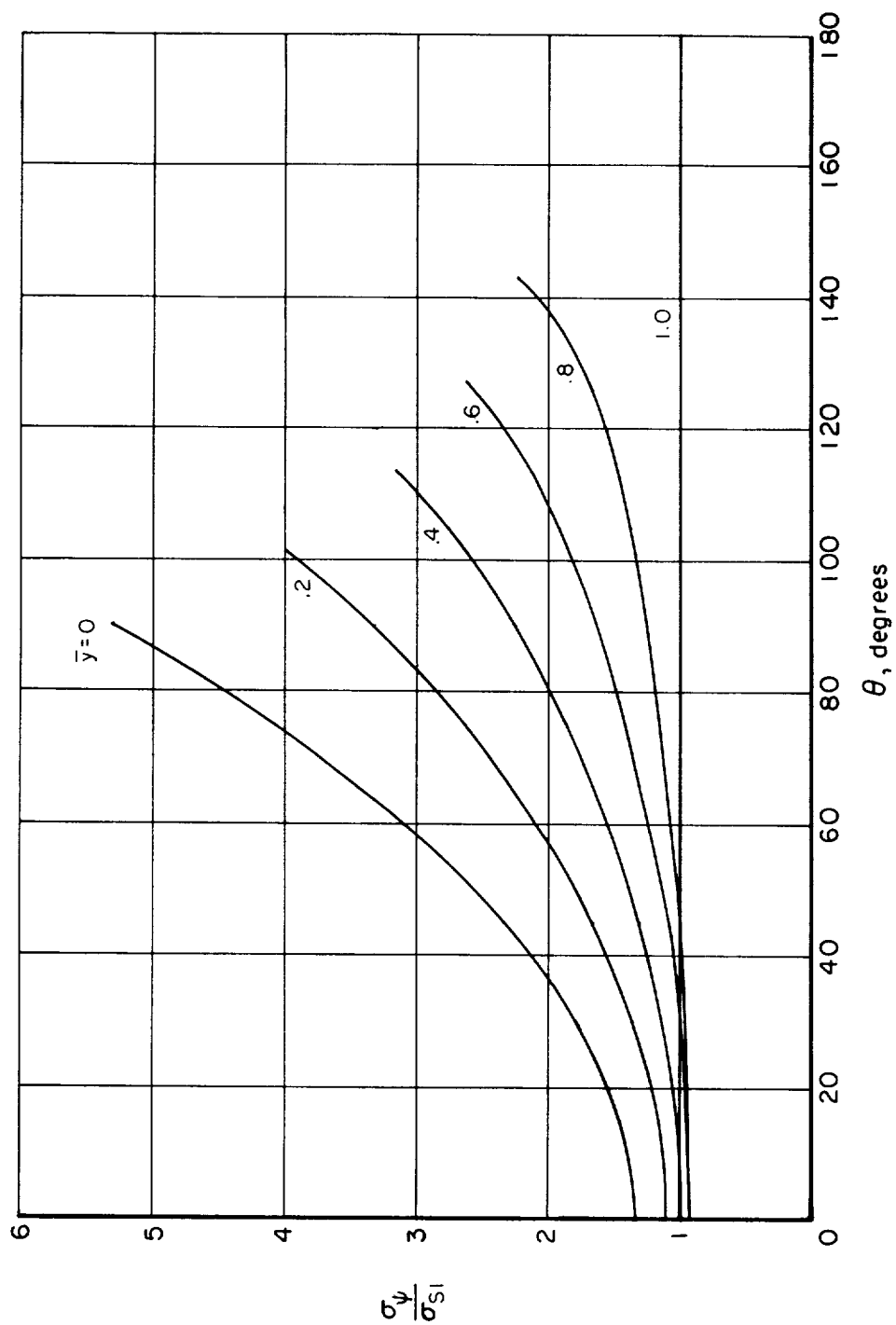
(d) Constant-area cords, $\mu_2(\sigma_{c2}/\rho_c) = 1.6 \times 10^8 \text{ ft}^2/\text{sec}^2$, $m_p/m = 0.4$, $\bar{y}_2 = 0.2$ ($-u_1 = 481.4 \text{ ft/sec}$).

Figure 1.- Continued.



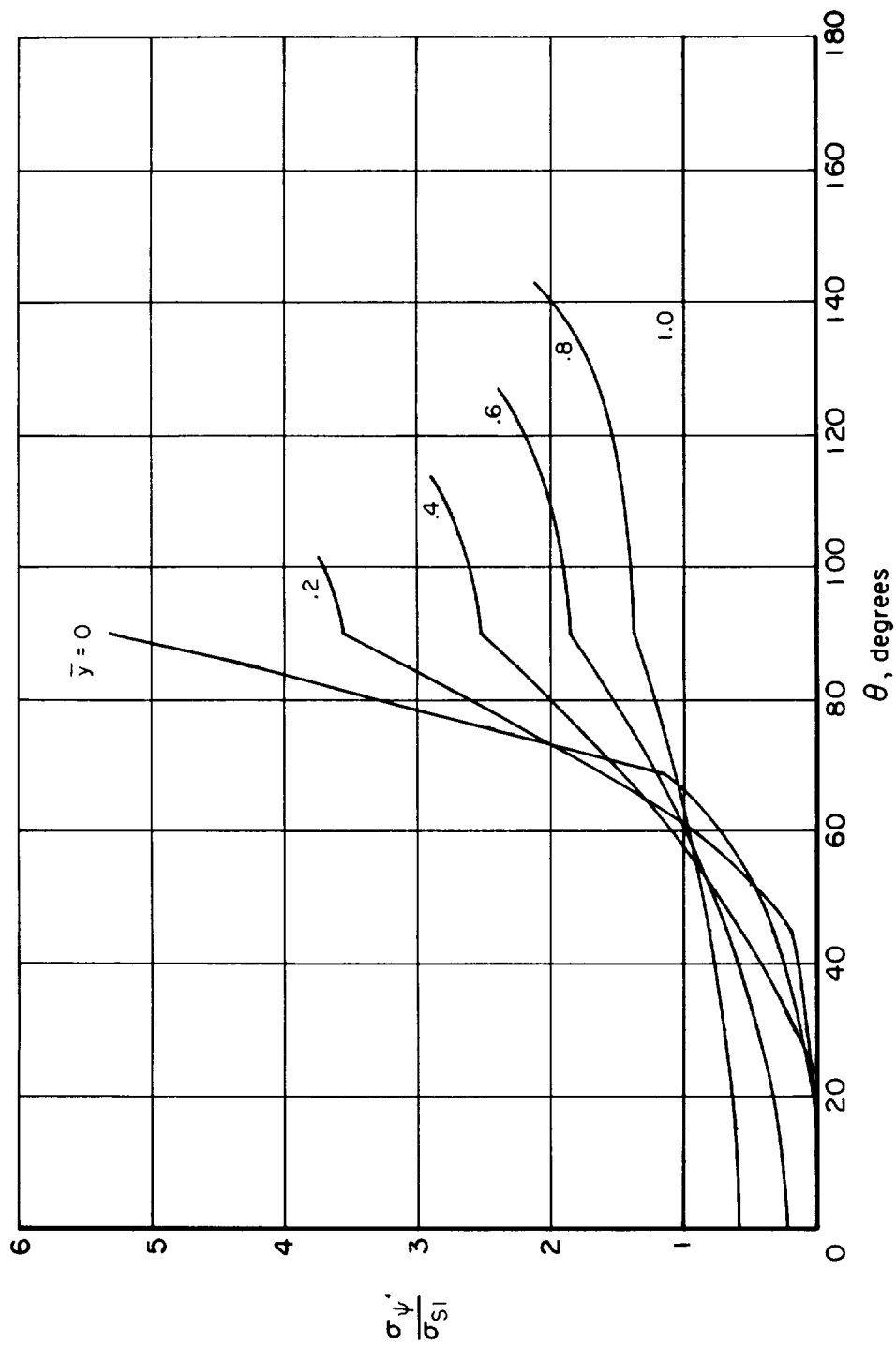
(e) Constant-area cords, $\mu_2(\sigma_{c2}/\rho_c) = 1.6 \times 10^8 \text{ ft}^2/\text{sec}^2$, $m_p/m = 0.6$, $\bar{y}_2 = 0.2$ ($-u_1 = 371.7 \text{ ft/sec}$).

Figure 1.- Concluded.



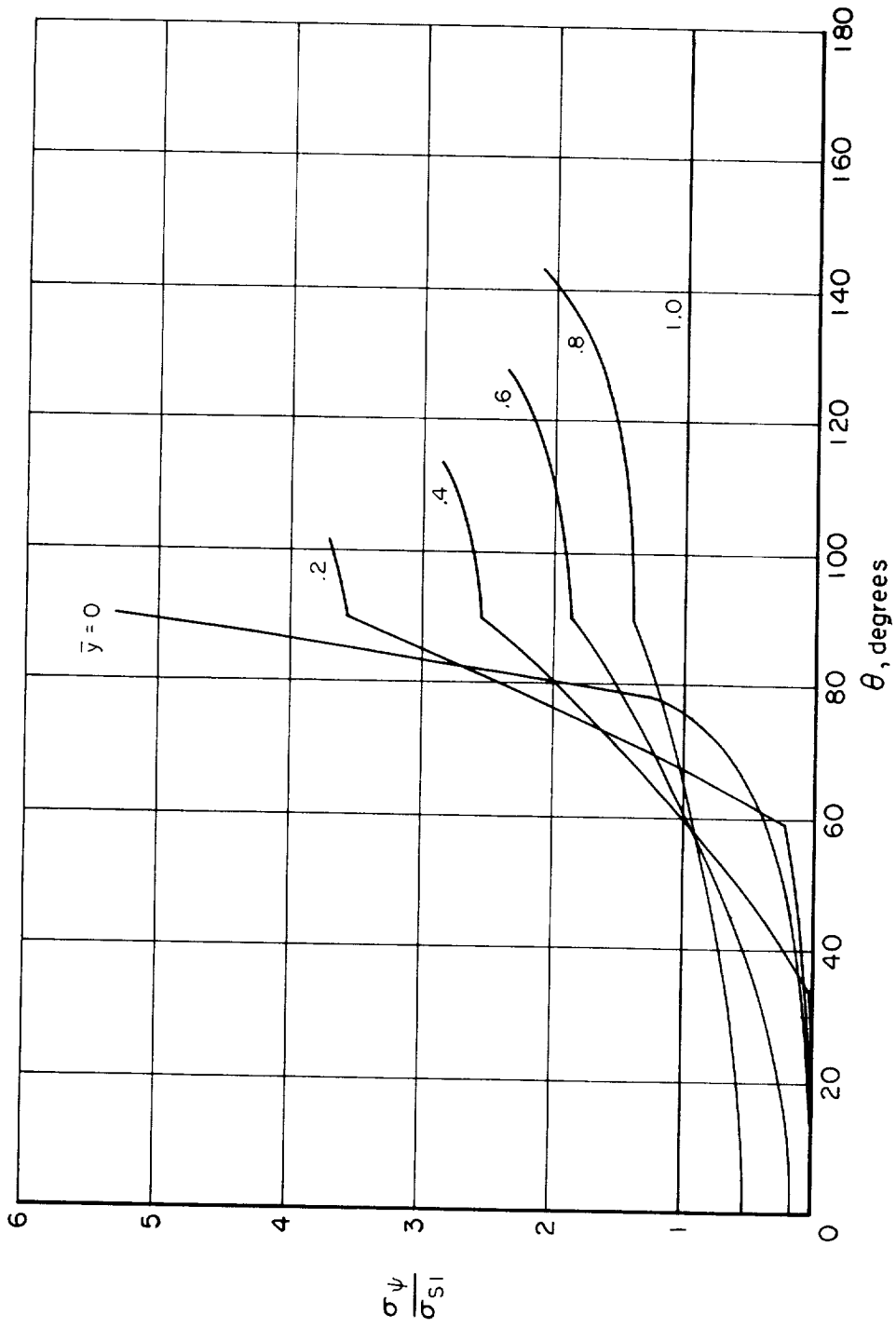
(a) $w_p/m = 0$, $w_c/m = 0$, $\bar{y}_2 = 0$ ($-u_1 = 1296.9$ ft/sec)

Figure 2.- Skin stress normal to a meridian (hydrogen inflating gas, $\bar{p}_a = 0$, $T_1 = 500^\circ R$, $\sigma_{S1}/\rho_S = 10^6$ ft²/sec²).



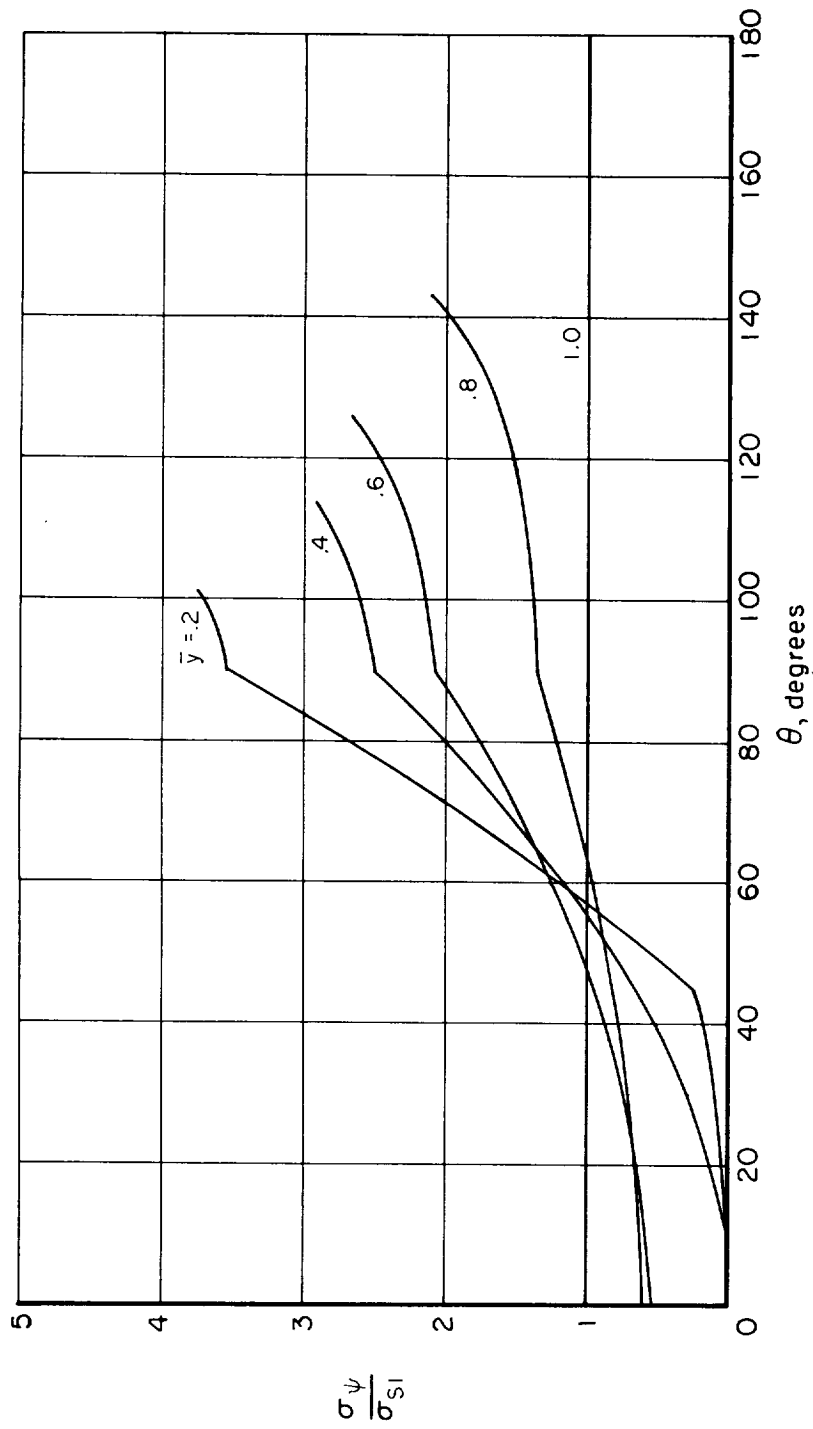
(b) Constant-area cords, $\mu_2(\sigma_{c2}/\rho_c) = 1.6 \times 10^8 \text{ ft}^2/\text{sec}^2$, $m_p/m = 0.4$, $\bar{y}_2 = 0$ ($-u_1 = 567.7 \text{ ft/sec}$).

Figure 2.- Continued.



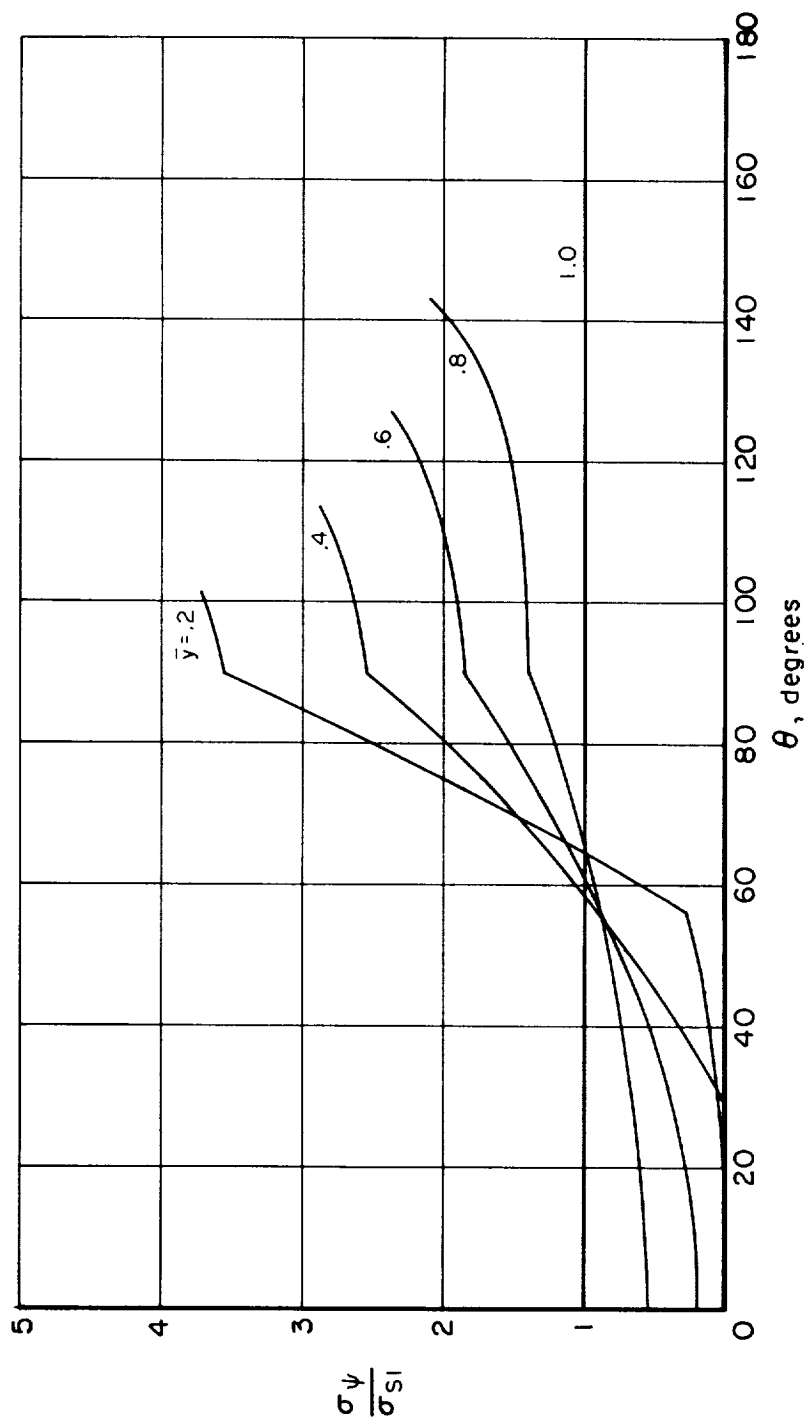
(c) Constant-area cords, $\mu_2(\sigma_{c2}/\rho_c) = 1.6 \times 10^6 \text{ ft}^2/\text{sec}^2$, $m_p/m = 0.6$, $\bar{y}_2 = 0$ ($-u_1 = 435.1 \text{ ft/sec}$).

Figure 2.- Continued.



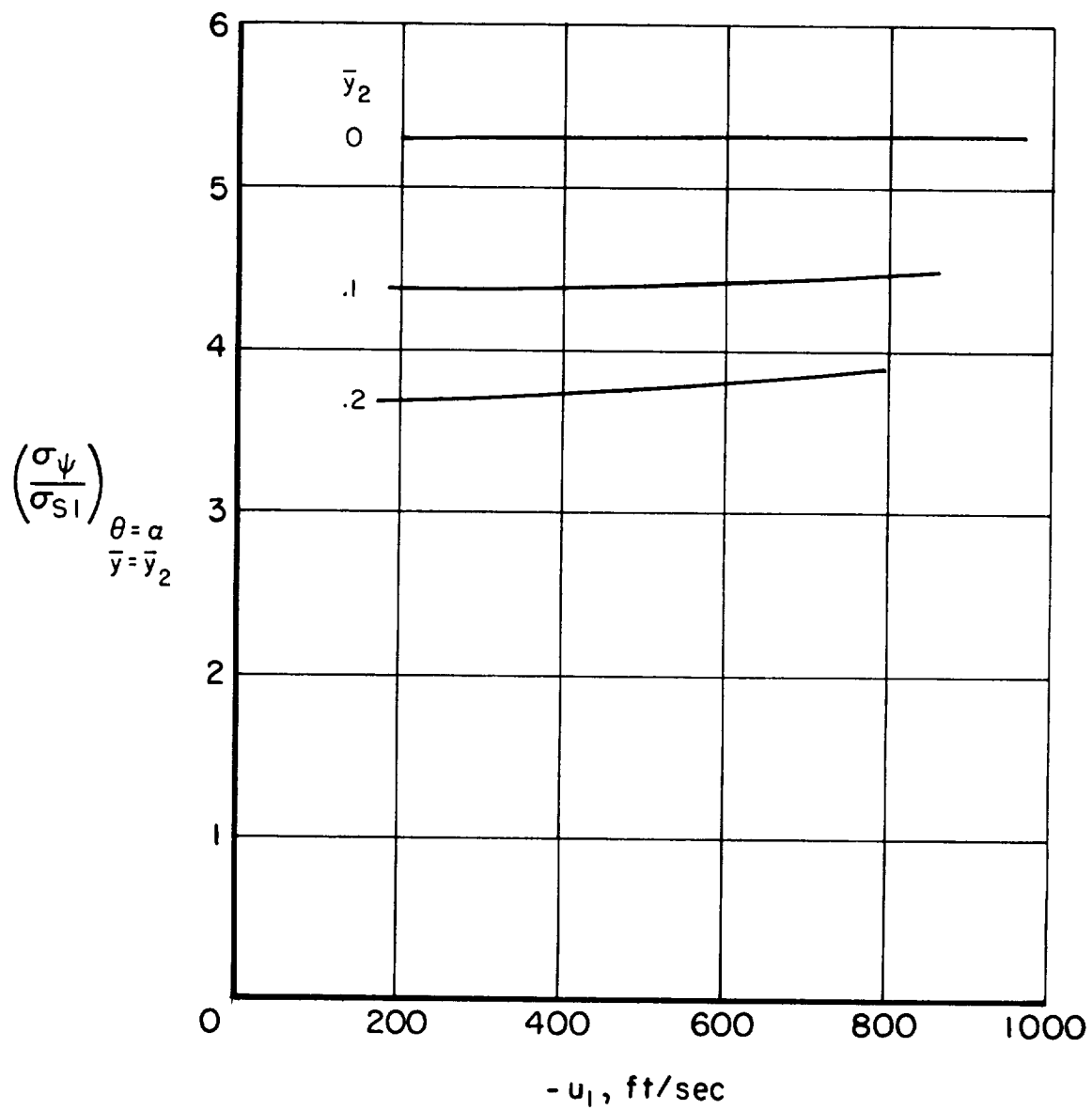
(d) Constant-area cords, $\mu_2(\sigma_{c2}/\rho_c) = 1.6 \times 10^6 \text{ ft}^2/\text{sec}^2$, $m_p/m = 0.4$, $\bar{y}_2 = 0.2$ ($-u_1 = 481.4 \text{ ft/sec}$).

Figure 2.- Continued.



(e) Constant-area cords, $\mu_2(\sigma_{c2}/\rho_c) = 1.6 \times 10^6 \text{ ft}^2/\text{sec}^2$, $m_p/m = 0.6$, $\bar{y}_2 = 0.2$ ($-u_1 = 371.7 \text{ ft/sec}$).

Figure 2.- Concluded.



(a) $\sigma_{s1}/\rho_B = 10^8 \text{ ft}^2/\text{sec}^2$

Figure 3.- Maximum skin stress (hydrogen inflating gas, $\bar{p}_a = 0$, $T_1 = 500^\circ \text{ R}$, constant-area cords, $\mu_2(\sigma_{c2}/\rho_c) = 1.6 \times 10^8 \text{ ft}^2/\text{sec}^2$).

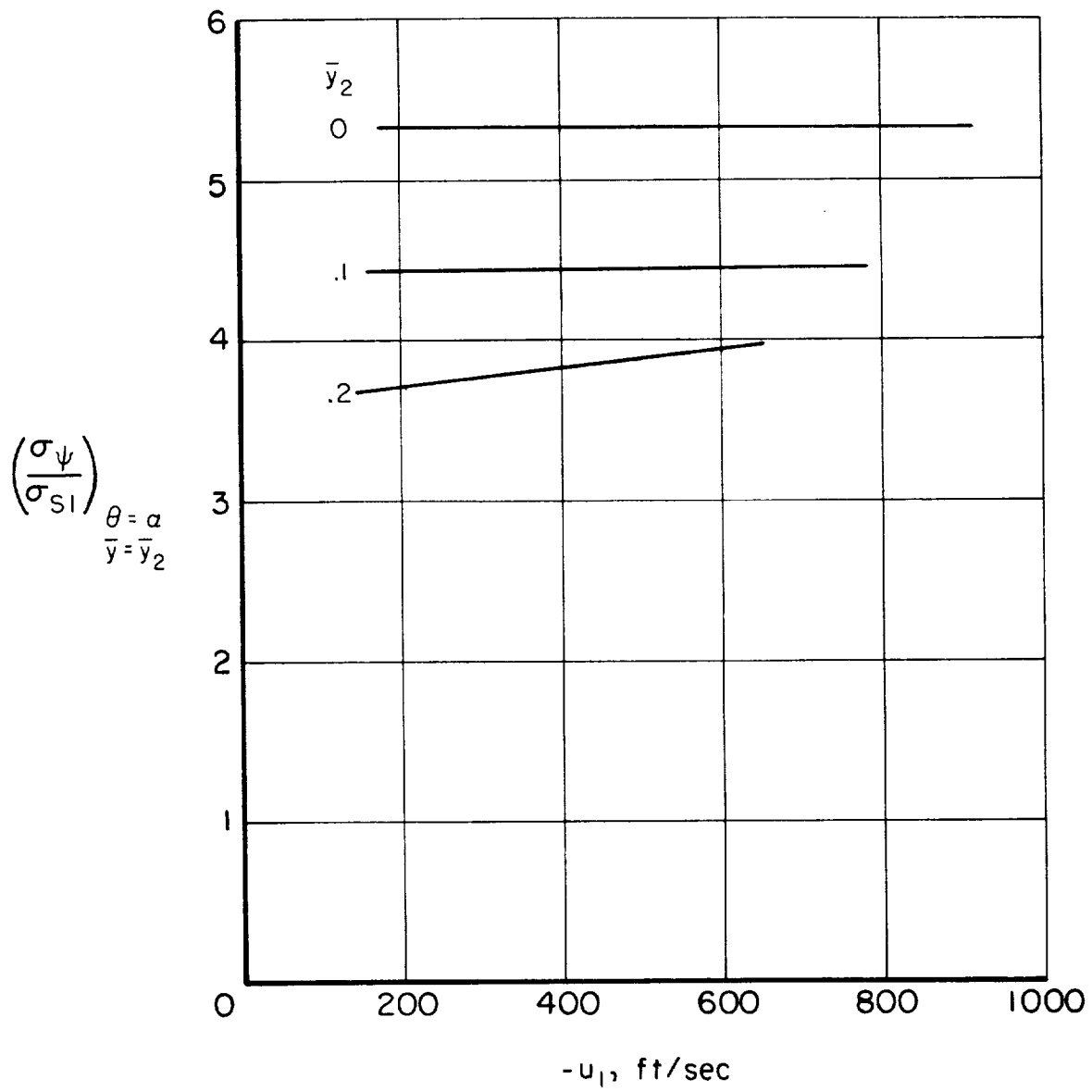
A
4
7
1(b) $\sigma_{s1}/\rho_s = 5 \times 10^5 \text{ ft}^2/\text{sec}^2$

Figure 3.- Concluded.

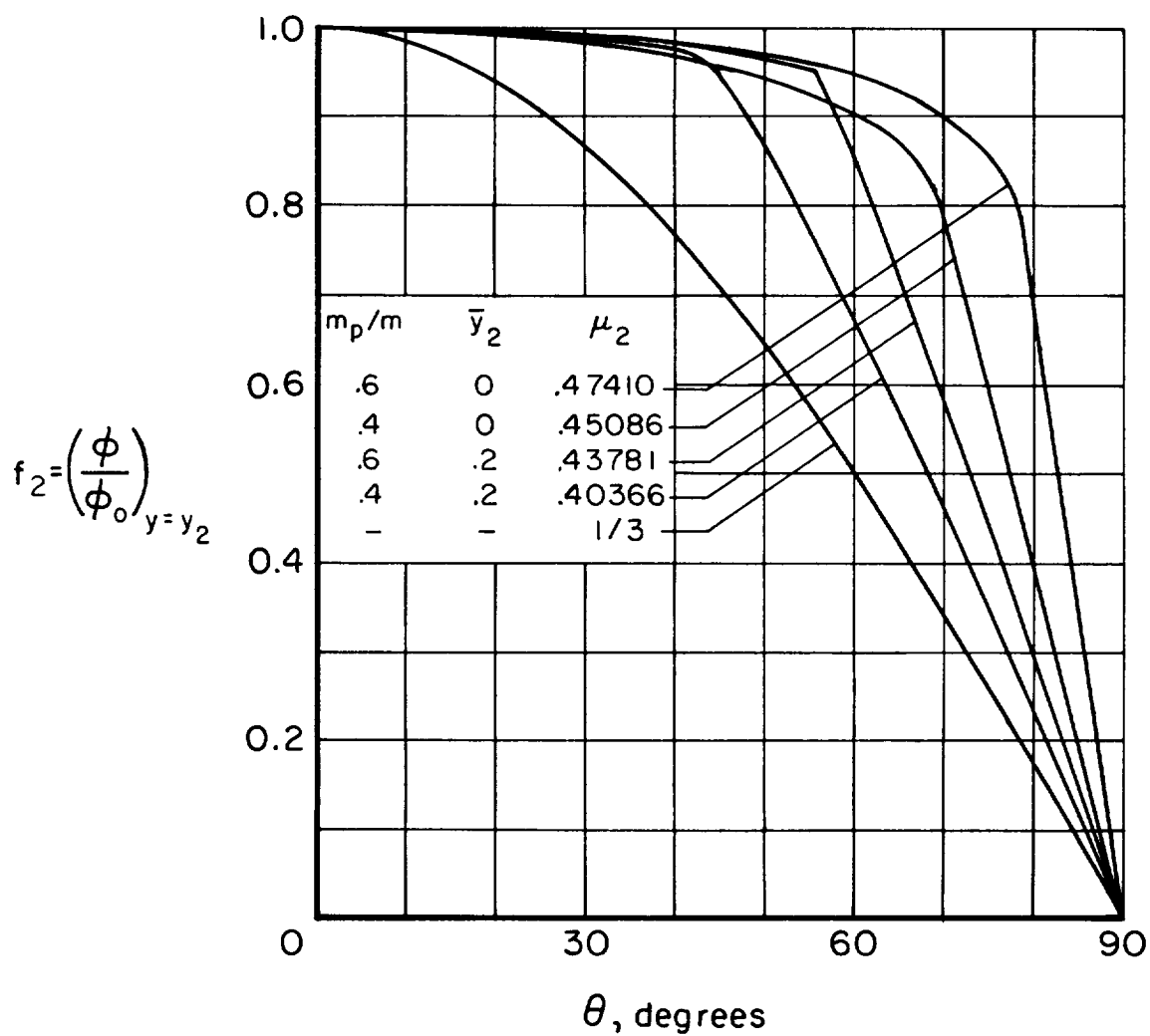


Figure 4.- Cord-force distributions (hydrogen inflating gas, $\bar{p}_a = 0$, $T_1 = 500^\circ \text{ R}$, $\sigma_{s1}/\rho_s = 10^6 \text{ ft}^2/\text{sec}^2$, constant area cords, $\mu_2(\sigma_{c2}/\rho_c) = 1.6 \times 10^6 \text{ ft}^2/\text{sec}^2$).

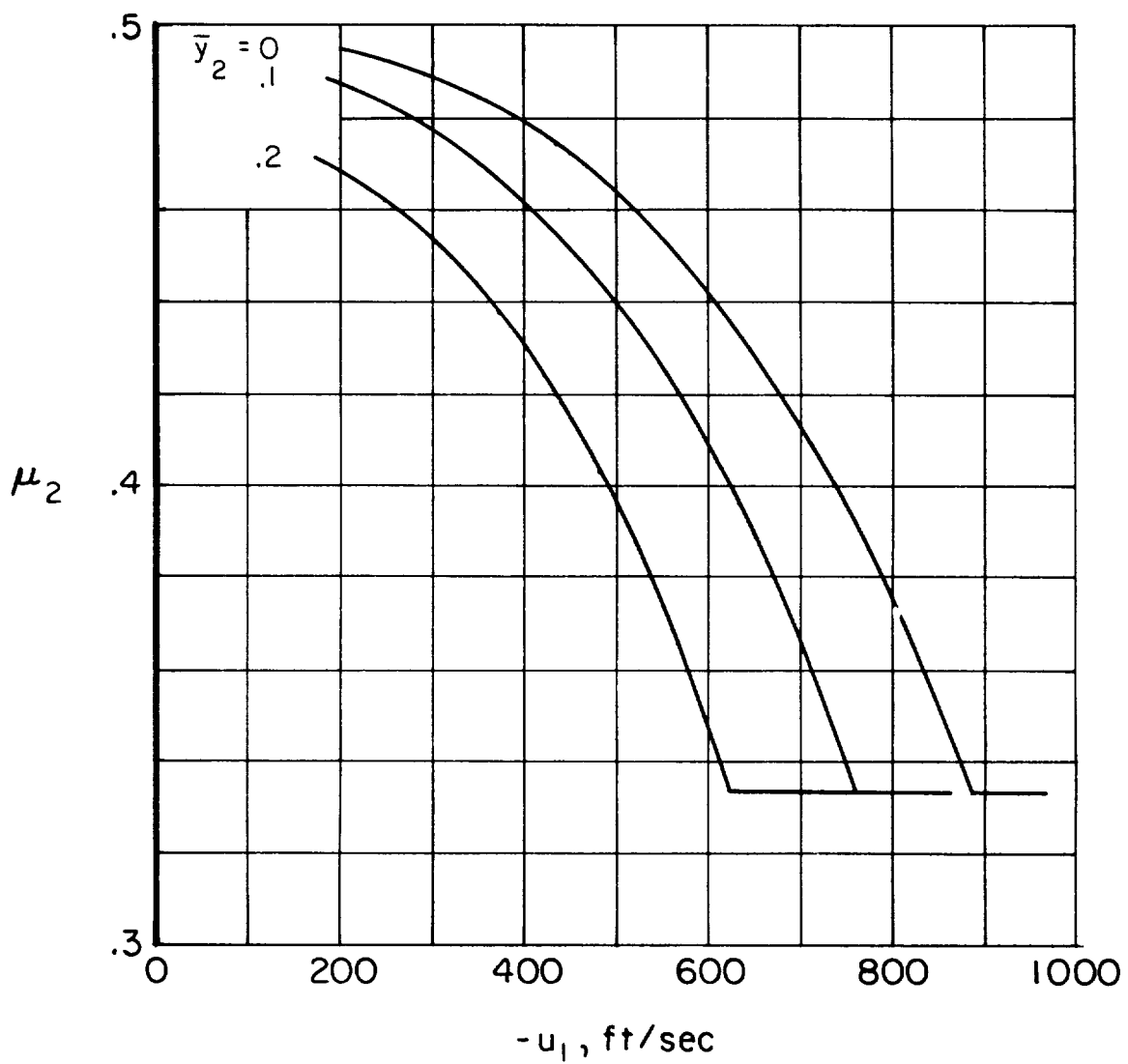


Figure 5.- Values of μ_2 corresponding to design cases (hydrogen inflating gas, $\bar{p}_2 = 0$, $T_1 = 500^\circ \text{R}$, $\sigma_{s1}/\rho_s = 10^6 \text{ ft}^2/\text{sec}^2$, constant-area cords, $\mu_2(\sigma_{c2}/\rho_c) = 1.6 \times 10^8 \text{ ft}^2/\text{sec}^2$).